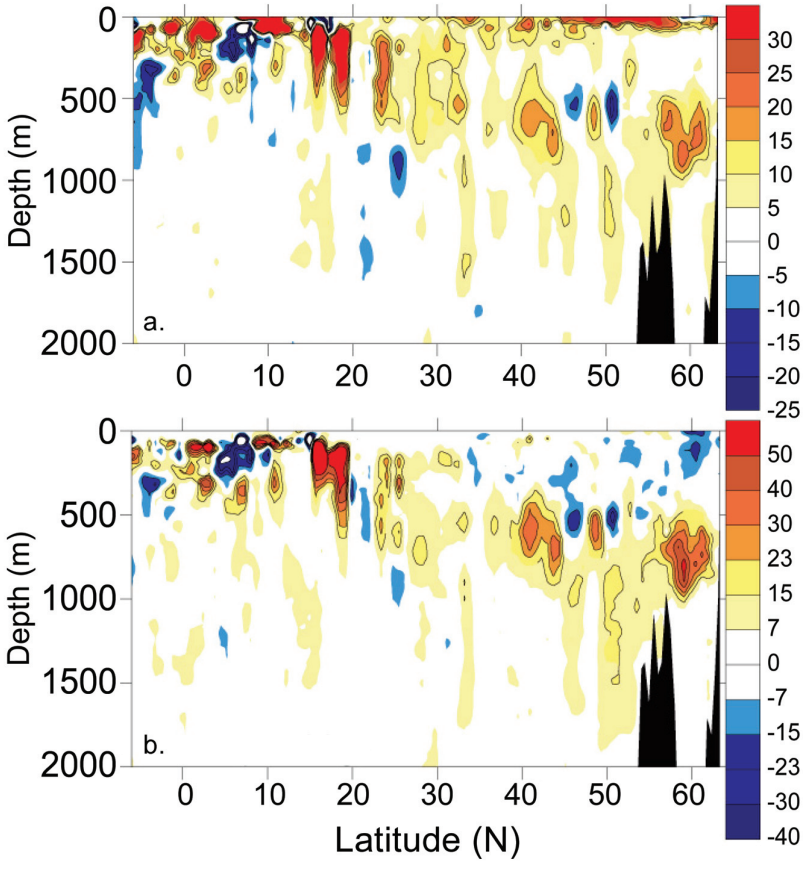

Fig. 3.13. Changes in (a) DIC (μmol kg^{-1}) and (b) AOU (μmol kg^{-1}) in the upper 2000 m between the 2003 and the 1993 occupations of A16N. Positive values are an increase in concentrations between 1993 and 2003 (modified from Feely et al. 2005).

ocean in the mid-1990s, these studies are unable to establish temporal and spatial scales of variability, or the temporal evolution of the ocean carbon cycle.

To address questions of decadal variability and temporal evolution, the U.S. Climate Variability and Predictability (CLIVAR) CO_2 Repeat Hydrography Program has identified 19 hydrographic sections distributed around the global ocean that will be re-occupied every 5–10 years. The program began in 2003 with three cruises in the North Atlantic that were repeats of cruises in the 1990s. Each year one to three cruises are run in different locations with a goal of completing the first global resurvey by 2012. In 2005, cruises were run in the South Atlantic and South Pacific Oceans, but these data will take several years to finalize and thoroughly examine.

Analysis of the initial repeat lines over this past year has indicated that several biogeochemical parameters are changing with time (Feely et al. 2005). For example, changes of –10 to +30 μmol kg^{-1} of DIC have been observed in the upper 1000 m of the water column between the 1993 and 2003 occupations of a track designated as A16N along 25°W in the North Atlantic (Fig. 3.13a). Although the magnitude of the changes is not surprising, the patchiness of the changes was not expected. More surprising is the fact that there have been similar changes in the apparent oxygen utilization (AOU) of the waters (a measure of the decomposition of organic matter in the ocean), indicating significant changes in the organic matter cycling over the last decade that was previously believed to be in steady state (Fig. 3.13b). The complicated patterns of these changes clearly show that carbon is being influenced by more than simple secular increases in atmospheric CO_2. In some cases changes in circulation and organic matter cycling may be masking anthropogenic changes, and in other cases these changes may enhance the apparent ocean carbon uptake.

Another intriguing preliminary finding from a comparison of a 2004 cruise in the North Pacific to the aforementioned North Atlantic results is that anthropogenic carbon inventories may be increasing in the Pacific at about twice the rate of the Atlantic over the last 10 years (Feely et al. 2005). This is in contrast to the long-term anthropogenic CO_2 inventory that shows larger column inventories in the North Atlantic. The interpretation of these recent findings may lie in understanding the effects of climate modes like the NAO or the Pacific Decadal Oscillation (PDO) on the decadal-scale circulation. These results also point to the need for improved approaches for isolating the anthropogenic and natural components of the observed variability.

4. THE TROPICS—H. J. Diamond[19] and K. A. Shein,[82] Eds.

a. Overview—H. J. Diamond[19]

This Tropics section consists of global input on two primary topics: 1) ENSO and the tropical Pacific, including ENSO seasonal variability, and 2) tropical cyclone activity for the 2005 season in the following seven basins: the Atlantic, northeast Pacific, northwest Pacific, North and South Indian,

southwest Pacific, and Australia. The Pacific ITCZ also is discussed.

Persistent anomalous rainfall that characterizes mature warm-phase ENSO conditions failed to develop near the date line, except in February 2005. The relative absence of such convection indicated that the ocean and atmosphere were only weakly coupled during this event. It should be noted that although conditions in the Pacific met the definition for El Niño according to the criterion recently formulated by the NOAA/National Centers for Environmental Prediction (NCEP), namely, five consecutive overlapping 3-month seasons with Niño-3.4 SST anomaly ≥ 0.5°C, this definition is not universally agreed upon, either because it is focused on a single region or defined only in terms of SST. Regarding tropical cyclone activity, while the 2005 season was unprecedented in the Atlantic, setting numerous records, other basins were characterized by near- to below-normal levels of activity. Two sidebars expand upon the record Atlantic basin tropical storm season.

b. El Niño–Southern Oscillation—G. D. Bell,[5] M. S. Halpert,[32] and M. J. McPhaden[53]

i) Overview

Conditions throughout the tropical Pacific during 2005 reflected a weak warm episode that ended in March, followed by the development of below-average SSTs during November and December (Fig. 4.1a). Intraseasonal variability often associated with the MJO also was present. The weak Pacific warm episode early in the year was accompanied by anomalously warm waters at approximately 110–130-m depths across most of the equatorial Pacific (Fig. 4.1b). Subsurface temperatures returned toward normal during April, before cooling during the following months.

The weak warm episode did not show a strong relationship to the 850-hPa zonal wind anomalies, which featured an oscillating pattern indicative of the MJO (Fig. 4.1c). However, a well-defined strengthening of the equatorial easterlies did accompany the transition to below-average SSTs during November and December. These enhanced easterlies also contributed to increased equatorial upwelling and a shoaling of the oceanic thermocline.

There was generally minor reflection of the anomalously warm SSTs in the pattern of deep convection over the central and east-central equatorial Pacific early in the year, as indicated by OLR anomalies (Fig. 4.1d). An El Niño signal was only evident during February, when convection was enhanced over the central equatorial Pacific (negative OLR anomalies) and suppressed across Indonesia early in the year.

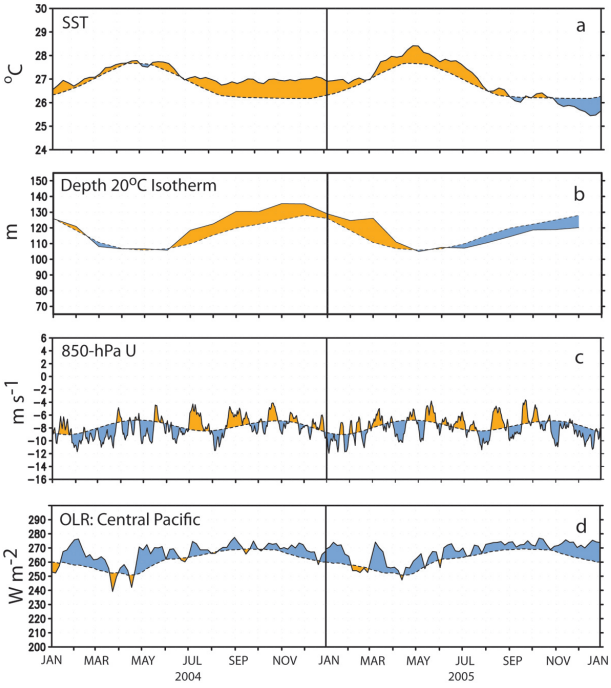

Fig. 4.1. Monthly time series of (a) SST (°C), (b) depth of the 20°C isotherm (m), (c) 850-hPa zonal wind speed (m s^{-1}), and (d) OLR (W m^{-2}) over the central equatorial Pacific. Values were averaged over the region bounded by 5°N–5°S and 180°–100°W. Five-day (solid line) and climatological (1979–95; dashed line) mean values are shown, as are positive (orange) and negative (blue) anomalies (except for OLR, where shading convention is reversed) relative to a 1979–95 base period.

This pattern impacted circulation over the Southern Hemisphere, likely resulting in the observed drop in rainfall across southern Africa during the heart of their rainy season.

Convection was slightly suppressed across the central equatorial Pacific for much of the year, and positive OLR anomalies became increasingly pronounced during November and December as the equatorial easterlies strengthened and SSTs dropped.

ii) The Madden–Julian oscillation, Kelvin wave activity, and atmospheric circulation

Low-frequency variability in the Tropics is strongly influenced by the MJO (Madden and Julian 1971, 1972, 1994), a tropical disturbance that modulates tropical convection and atmospheric circulation patterns with a typical period of 30–60 days. The MJO tends to be most active during ENSO-neutral years, and can produce ENSO-like anomalies (Mo and Kousky 1993; Kousky and Kayano 1994). Low-level (850 hPa) and upper-level (200 hPa) equatorial zonal winds and streamfunction, 200-hPa velocity potential

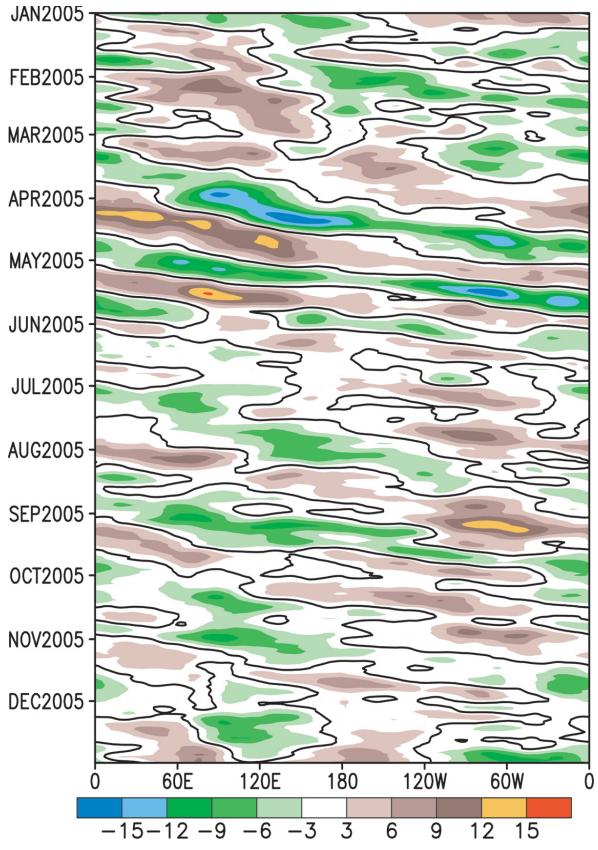

Fig. 4.2. Time–longitude section (5°N–5°S) of daily 200-hPa velocity potential anomalies ($m^2\ s^{-1}$) during 2005. The shading interval is $3 \times 10^6\ m^2\ s^{-1}$, and the thick solid contour is the zero line. Anomalies are departures from the 1971–2000 base period daily means, and plotted using a 5-day running mean smoother.

and tropical convection, and both sea surface and subsurface temperature anomalies exhibited considerable intraseasonal variability during 2005 in association with the MJO.

The MJO is indicated in a time–longitude section by continuous propagation of the 200-hPa velocity potential anomalies around the globe (Fig. 4.2). Periods when the MJO was active include March–May and July–September. This MJO activity contributed to alternating periods of enhanced and suppressed convection from the Indian Ocean to the date line, and to alternating periods of low-level easterly and westerly wind anomalies across the tropical Pacific (Fig. 4.1c).

The low-level wind anomalies associated with the MJO can generate eastward-propagating oceanic Kelvin waves, typically traveling 10° longitude $week^{-1}$, that feature downwelling in the mixed layer at their leading edge and upwelling in their wake (Zhang et al. 2001). Major Kelvin waves occurred during March–May in response to very strong westerly wind bursts over the western equatorial Pacific linked to the MJO (Fig. 4.3). As indicated by a time series of area-averaged SST anomalies in the Niño-3 region, the upwelling phase of one Kelvin wave produced a marked drop in SSTs across the east-central equatorial Pacific during February, followed by a return to near-normal SSTs in March (Fig. 4.4). The downwelling phase of a second Kelvin wave reached the region in early May, causing an abrupt increase in SSTs to 0.9°C above average. These anomalies exceeded earlier values associated with the weak warm episode. Several ENSO forecast models interpreted this anomalous warming as an indication of a possible return to El Niño conditions. However, the upwelling phase of the MJO followed behind, which dissipated the warmth soon thereafter.

An unusual feature of this El Niño was that excess heat content along the equator, typically a precursor to subsequent ENSO SST anomaly development (Jin 1997, Meinen and McPhaden 2000), did not precede but rather developed in phase with Niño-3.4 SST anomalies during 2004/05 (Fig. 4.5). The lack of a subsurface heat content precursor may account for the relative weakness of the 2004/05 El Niño and the difficulty in predicting its onset (Lyon and Barnston 2005). By the end of 2005, the excess equatorial heat

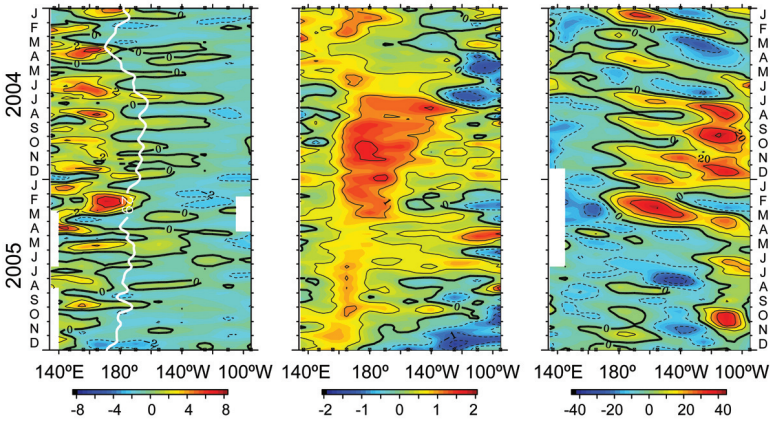

Fig. 4.3. Five-day average anomalies of (left) zonal wind ($m\ s^{-1}$), (center) SST (°C), and (right) 20°C depth (m; an index for the depth of the thermocline) relative to the mean seasonal cycle averaged over 2°N–2°S based on TAO/TRITON moored time series data. The white line on the left panel indicates the 29°C isotherm, which marks the eastern edge of the western Pacific warm pool. Ticks on the horizontal axis indicate longitudes sampled at the start (top) and end (bottom) of record.

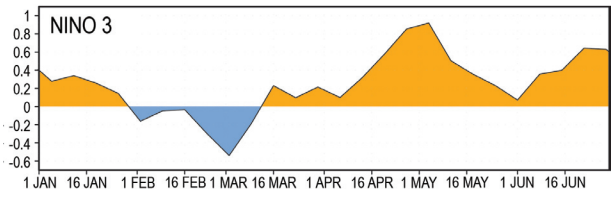

Fig. 4.4. Time series of the Niño-3 region SST anomaly index calculated over the area (5°N–5°S, 90°–150°W).

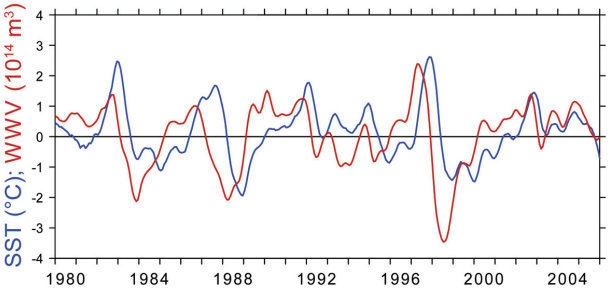

Fig. 4.5. Monthly anomalies of Niño-3.4 SST (°C) and warm water volume (WWV; × 10^{14} m^3) from January 1980 to December 2005. WWV, which is an index of heat content along the equator, is based on a blended thermal field analysis of TAO/TRITON moored time series data and ship-of-opportunity expendable bathythermograph (XBT) data integrated over the region of 5°N–5°S, 80°W–120°E above the 20°C isotherm. Niño-3.4 SST represents an average anomaly over the region of 5°N–5°S, 120°–170°W. Time series have been smoothed with a 5-month running mean filter.

content prevalent during most of 2004/05 had disappeared in association with the onset of cold La Niña conditions (Fig. 4.5).

Anomalous warming associated with the El Niño–like conditions during 2004/05 was centered near the date line. Conversely, near-normal SSTs prevailed in the eastern Pacific and along the west coast of South America. The failure of persistent warm SST anomalies to develop in the eastern equatorial Pacific and along the west coasts of the Americas limited the effects of this El Niño on marine ecosystems and fisheries in those regions.

c. *Tropical cyclones*

i) Seasonal activity overview—H. J. Diamond[19] and D. H. Levinson[46]

Averaged across all basins, the tropical storm seasons of 2005 (2004/05 in the Southern Hemisphere) saw an above-normal number of named storms relative to the 1981–2000 mean. Of these, fewer than normal became hurricanes/typhoons/cyclones (HTCs), but the number of major HTCs was slightly above average. Globally, 103 tropical storms (≥ 34 kt) were recorded, with 53 becoming HTCs (≥ 64 kt), and 28 attaining major/intense (≥ 96 kt) status (compared to an average of 97.25, 55, and 25.35 storms, respectively). The 2005 season was unprecedented in the Atlantic, with numerous seasonal and individual storm-related records. The highlights in the Atlantic included the existence of three Saffir–Simpson category 5 storms (e.g., Wilma; Fig. 4.6), which are discussed in a sidebar on the Atlantic season. While the Atlantic had its all-time busiest season ever with 27 total storms (see note in abstract), other basins were characterized by near- to below-normal levels of activity.

ii) Atlantic basin—G. D. Bell,[5] E. Blake,[8] K. C. Mo,[58] C. W. Landsea,[44] R. Pasch,[65] M. Chelliah,[15] and S. B. Goldenberg[29]

The tropical multidecadal signal incorporates the leading modes of tropical convective rainfall variability occurring on multidecadal time scales. Three important aspects of this signal responsible for the increased hurricane activity since 1995 are 1) a stronger West African monsoon system; 2) suppressed convection in the Amazon Basin; and 3) the warm phase of the Atlantic multidecadal mode (Goldenberg et al. 2001; Bell and Chelliah 2006). This tropical multidecadal signal is very important to Atlantic hurricanes because it affects an entire set of critical conditions across the main development region (MDR) for decades at a time. The MDR consists of the tropical Atlantic and Caribbean Sea south of 21.5°N (Fig. 4.7a, green box). During 2005,

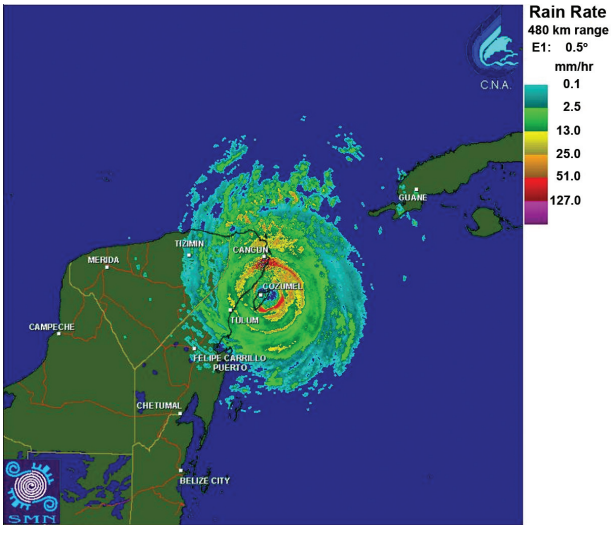

Fig 4.6. Mexican Meteorological Service radar image of category 5 Hurricane Wilma striking the Yucatan Peninsula on 21 Oct 2005. [Source: Servicio Meteorologico Nacional]

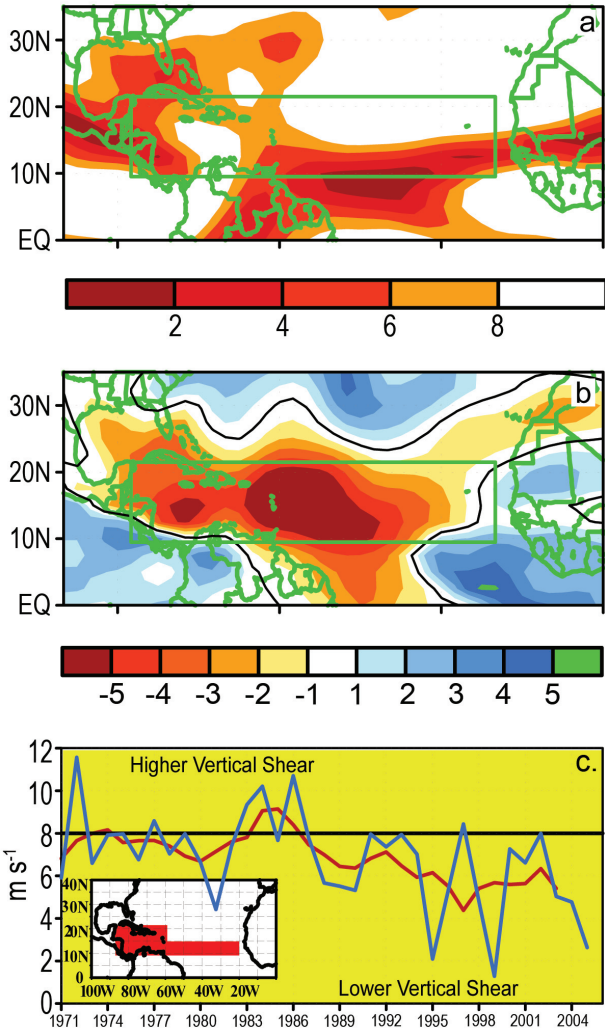

Fig. 4.7. June–October (a) 200–850-hPa vertical wind shear magnitude total (m s^{-1}) and (b) anomalies. In (a) only values less than 8 m s^{-1} are shaded. In (b) red shading indicates below-average strength of the vertical shear. Green box denotes the MDR. Anomalies in (b) are departures from the 1971–2000 base period monthly means. (c) A time series of August–October area-averaged 200–850-hPa vertical shear of the zonal wind (m s^{-1}) across the MDR (inset). Blue curve shows unsmoothed 3-month values, and red curve shows a 5-point running mean applied to the time series.

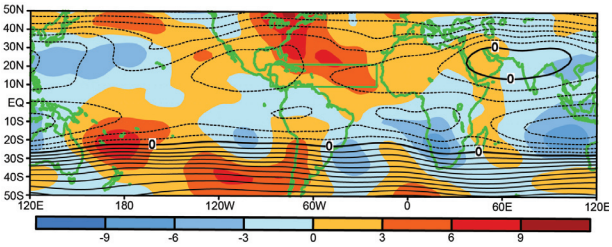

Fig. 4.8. June–October 2005 mean (contours, interval is 10 × 10^6 m^2 s^{-1}) and anomalous (shading) 200-hPa streamfunction. Anticyclonic anomalies are indicated by positive values in the NH and negative values in the SH. Cyclonic anomalies are indicated by negative values in the NH and positive values in the SH. Anomalies are departures from the 1971–2000 base period monthly means. Green box denotes the MDR.

this signal again set the backdrop for many of the observed atmospheric and oceanic anomalies. The 2005 hurricane season featured an extensive area of low vertical wind shear (less than the 8 m s^{-1} threshold for tropical cyclone formation) throughout the MDR and Gulf of Mexico (Fig. 4.7a), with the largest anomalies centered over the central tropical Atlantic and Caribbean Sea (Fig. 4.7b). Since 1995, the area-averaged vertical shear in the heart of the low-shear area has been approximately 5–6 m s^{-1}, with values during individual years such as 2005, 1999, and 1995, dropping to an incredibly low 2 m s^{-1}.

This extensive area of low shear in 2005 resulted in part from a stronger-than-average tropical easterly jet and an expanded area of upper-level easterly winds across the western MDR, both of which were related to an enhanced subtropical ridge at 200 hPa. The 200-hPa streamfunction field (Fig. 4.8) shows that these conditions were part of a larger-scale pattern during 2005, characterized by anticyclonic anomalies (Fig. 4.8; red in NH, blue in SH) and enhanced subtropical ridges in both hemispheres from the eastern Pacific to Africa, and by cyclonic anomalies in both hemispheres over the central tropical Pacific. This Tropics-wide pattern with its pronounced interhemispheric symmetry is a classic signature of very active Atlantic hurricane seasons. Bell and Chelliah (2006) indicate that this pattern signifies a response to anomalous tropical convection, partly related to the ongoing tropical multidecadal signal, and partly related to suppressed convection over the central equatorial Pacific.

During 2005, long periods of anomalous upper-level convergence were evident over the central tropical Pacific, with shorter-period fluctuations sometimes related to the MJO (Fig. 4.9, solid line). Throughout the season, these periods of suppressed convection led to a strengthening of the 200-hPa subtropical ridge over the western North Atlantic (Fig. 4.9, orange shading), which acted to focus periods of TC activity. For example, 10 of the season's 15 hurricanes and all 7 major hurricanes formed during these periods. All seven early season TCs and two mid-November TCs also occurred when convection was suppressed near the date line. This finding is consistent with the study of Mo (2000). Also consistent with that study is the break in activity during the first half of August in association with MJO-related enhanced convection near the date line.

The low vertical shear during 2005 was also associated with westerly wind anomalies in the lower troposphere that reflected a markedly reduced strength of the tropical easterly trade winds from the eastern tropical Pacific to Africa. In combination with the anomalous upper-level easterlies, this wind distribution is consistent with the baroclinic response of the atmospheric circulation to anomalous tropical convection linked in part to the tropical multidecadal signal (Bell and Chelliah 2006). Over the Caribbean Sea, the weaker easterly trade winds corresponded with exceptionally low SLP and 1000-hPa heights in response to a weakening and northeastward shift of the Bermuda high. These conditions were associated with anomalous low-level cyclonic vorticity across the northern half of the MDR, western North Atlantic, and Gulf of Mexico.

These favorable conditions extended up to 700 hPa along the equatorward flank of the African easterly jet (AEJ) (Fig. 4.11). The associated anomaly patterns at this level are also consistent with the ongoing tropical multidecadal signal. Conversely, during the preceding period (1971–94) of below-normal activity, higher vertical shear (Fig. 4.7b), combined with stronger easterly trade winds and reduced cyclonic vorticity south of the AEJ axis, were not conducive to Atlantic hurricane formation in the MDR.

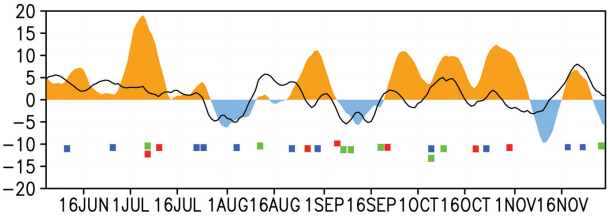

Fig. 4.9. Five-day running mean time series showing area-averaged anomalies of 200-hPa velocity potential (line) and 200-hPa streamfunction (shading) during 10 Jun–30 Nov 2005 ($m^2 s^{-1}$). Velocity potential anomalies are calculated for the central tropical Pacific region bounded by 10°–20°N, 160°E–170°W. Streamfunction anomalies are calculated for the Gulf of Mexico and Caribbean Sea bounded by 10°–30°N, 60°–100°W. Small boxes below time series indicate when tropical storms (blue), Category 1–2 hurricanes (green), and major hurricanes (red) formed in the Atlantic basin. Anomalies are departures from the 1971–2000 period daily means.

Favorable lower-level conditions during 2005 were also associated with record warm SSTs across the tropical Atlantic, Caribbean Sea, and Gulf of Mexico (Fig. 4.12, top). For the entire season SSTs across the western tropical Atlantic and Gulf of Mexico reached an 1870–2005 all-time high of 28.7°C (Fig. 4.12, bottom). The above conditions meant that African easterly waves were embedded within an extended

ATLANTIC MONTHLY AIR–SEA FLUXES AND THE 2005 HURRICANE SEASON—M. A. Bourassa,[9] S. R. Smith,[84] P. Hughes,[33] and J. Rolph[76]

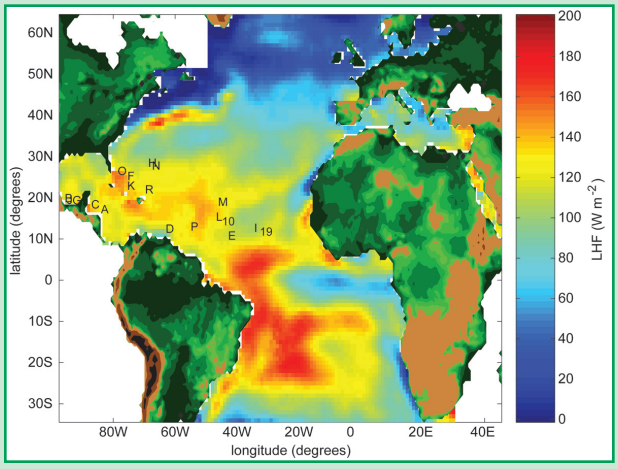

Fig. 4.10. Model-derived latent heat fluxes ($W m^{-2}$) during June–September 2005. The first letters of named storms are located where the storm was first named. The numbers indicate similar positions for tropical depressions that did not become named storms.

Latent heat flux refers to the rate at which water vapor energy is transferred from the ocean to the atmosphere. The release of this energy occurs at higher altitudes in association with deep convective clouds, and is a critical energy source for developing tropical cyclones. The latent heat flux during 2005 was estimated using a newly completed version of The Florida State University air–sea flux fields (FSU3; Bourassa et al. 2005). The objectively analyzed latent heat fluxes across the tropical Atlantic were generally 100–140 W m^{-2} during June–September, with larger values coinciding with tropical cyclone genesis regions (Fig. 4.10). The area-averaged anomalous latent heat flux during the period was 10 W m^{-2}, which is 20% greater than the largest value in the 1978–2003 time series (not shown). It is suggested that this increased latent heat flux, combined with above average SSTs and a strong cross-equatorial flow of deep tropical moisture into the heart of the MDR, led to a more unstable and deeper boundary layer that favored increased tropical cyclone activity.

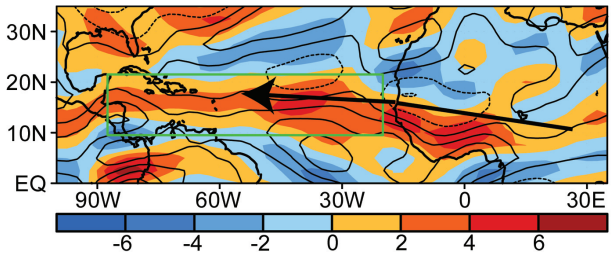

Fig. 4.11. June–October 2005 700-hPa anomalous zonal winds (contour interval is 1.0 m s^{-1}) and relative vorticity (shading, × 10^{-6} s^{-1}). Solid (dashed) contours indicate westerly (easterly) winds. Yellow-red (blue) shading indicates anomalous cyclonic (anticyclonic) relative vorticity. Arrow shows mean position of the African easterly jet axis during August–October. Green box denotes the MDR. Anomalies are departures from the 1971–2000 base period monthly means.

region of anomalous cyclonic vorticity as they moved westward over very warm SSTs into the low-shear, low-SLP, high-vorticity environment of the central and western MDR. This combination is known to favor very active hurricane seasons (Bell et al. 1999, 2000 2004; Lawrimore et al. 2001).

While the combination of the supportive multidecadal signal and suppressed convection near the date line established an environment conducive for a very active season, these factors cannot account for periods when atmospheric anomalies were exceptionally strong. They also cannot account for the propensity of many TCs to develop in and around, or traverse the Gulf of Mexico. Three additional factors likely contributed to these conditions. The first was a northeastward shift and strengthening of the ITCZ over the eastern North Pacific, with a corresponding increase in convection over Central America and southern Mexico. Associated with this pattern, an extensive area of low SLP over the Gulf of Mexico contributed to periods of actual low-level westerly winds across the Caribbean Sea, which further strengthened the low-level cyclonic circulation over the Gulf of Mexico. Second was a persistent ridge of high pressure in the middle and upper troposphere over the southeastern United States and Gulf regions, which can be linked to large-scale extratropical anomaly patterns (Fig. 4.9), and contributed to the low vertical shear across the Gulf of Mexico and western MDR. This ridge was particularly strong in July (Fig. 4.8), when it contributed to a sharp drop in vertical shear across the southern and western MDR. Three hurricanes formed in the MDR during this period, with two becoming major hurricanes. Last, above-average SSTs in an already very warm Gulf of Mexico (Fig. 4.12, top) made the environment over the western Atlantic and Gulf of Mexico even more conducive to tropical cyclogenesis and major hurricane formation. In effect, the environment in these regions during much of the season typified the central MDR during an active season. South of the anomalous upper-level ridge over the eastern United States, enhanced easterly flow also helped to steer many of the developing TCs into the Gulf of Mexico, all of which eventually made landfall.

Finally, the failure of many tropical storms to develop until they reached the western part of the basin is related to a pronounced eastward shift of the mean upper-level trough to the extreme eastern North Atlantic (Fig. 4.8). This shift occurred in association

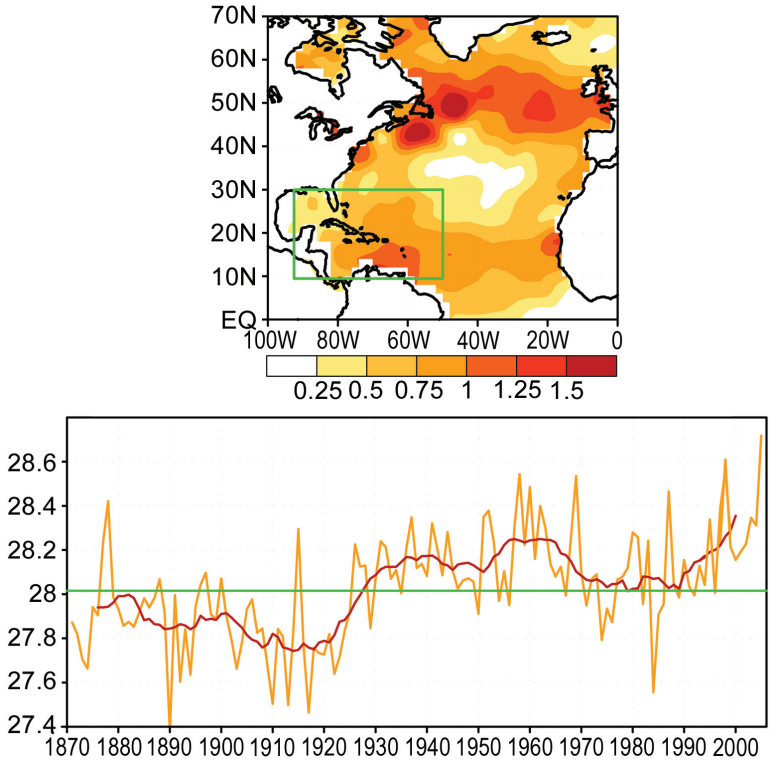

Fig. 4.12. Seasonal June–November (top) SST anomalies (°C) during 2005 and (bottom) time series of area-averaged SSTs (°C) in the (top) green boxed region. (bottom) Red line shows the corresponding 11-yr running mean. Averaging region corresponds to where seasonal activity was heavily focused during 2005.

with the persistent upper-level ridge farther west, and resulted in periods of anomalous upper-level westerlies and increased vertical wind shear that suppressed tropical wave development in the eastern MDR.

iii) East Pacific basin—D. H. Levinson[46]

(i) Overview of the 2005 season

The hurricane season in the eastern North Pacific (ENP) basin typically begins in mid-May and runs through the end of November, with a climatological peak in September. The 2005 hurricane season in the ENP was below normal, with the majority of the activity in the basin occurring during August and September. A total of 15 named storms (NSs), 7 hurricanes (Hs), and 2 major hurricanes (MHs) developed in the ENP basin in 2005, which was less than the NOAA National Hurricane Center (NHC) 1971–2003 seasonal climatology of 15.5 NSs, 9 Hs, and 4.3 MHs. A tropical depression (TD) formed in mid-October (TD 16-E), and was relatively long lived, but did not intensify to tropical storm strength. In addition to the total number of tropical cyclones, the 2005 ENP hurricane season was also below average for landfalling systems along the Pacific coast of Mexico.

(ii) Comparison of the 2005 season with climatology

The variability of ENP tropical cyclone activity is summarized with several widely used parameters and indices (Figs. 4.13a–d). In terms of the number of NSs, which is the total number of tropical cyclones that reach at least minimal tropical storm strength (sustained winds ≥ 34 kt), activity in the ENP basin has been near average since the mid-1990s, fluctuating between slightly above or below the long-term

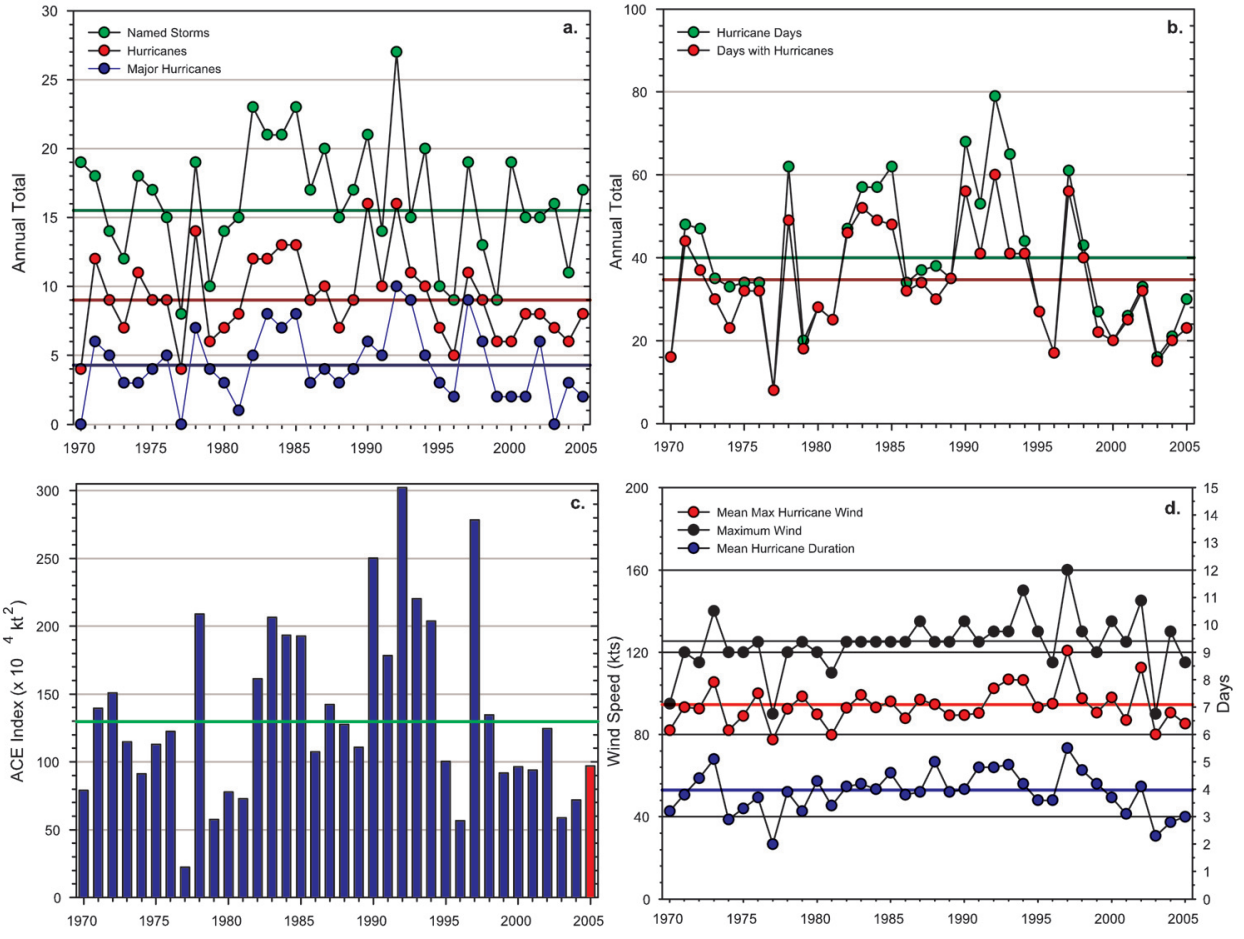

Fig. 4.13. Seasonal tropical cyclone statistics for the east North Pacific Ocean over the period 1970–2005: (a) number of NSs, Hs, and MHs, (b) days with hurricanes (the number of days with winds ≥ 64 kt) and hurricane days (days with winds ≥ 64 kt times the number of storms with winds ≥ 64 kt), c) the Accumulated Cyclone Energy (ACE) Index (× 10^4 kt^2) with 2005 highlighted in red, and d) the maximum and mean maximum wind speed (kt), and mean hurricane duration (days). All time series in (a)–(d) include the corresponding 1971–2003 base period means.

mean of 15.5 yr^{-1} (Fig. 4.13a). However, the annual number of hurricanes and major hurricanes have been below average in most years since 1995, except for the El Niño years of 1997/98. In addition, there were no landfalling named systems during the 2005 ENP season.

Despite the obvious importance of the number of tropical cyclones in any particular year, several other indices are useful in determining the historical significance of an individual hurricane season. Figure 4.13b shows this activity in terms of the annual number of days with hurricanes as well as hurricane days, and both of these statistics have been below average since 1995, again with the exception of the 1997/98 El Niño years.

In recent years, the Accumulated Cyclone Energy (ACE) Index (Bell et al. 2000) has been used as a diagnostic tool for understanding the intensity and duration of tropical cyclone activity. The ACE Index value for the ENP basin in 2005 was approximately 97 $\times 10^4$ kt^2, which was below both the long-term mean and median, and also within NOAA's definition of a "below normal" season. Historically, the ENP basin had a well-defined peak in the ACE Index during the early 1990s, with the highest annual value occurring in 1992. With the exception of 1997, there has been a marked decrease in the ACE Index for the ENP basin beginning in 1995. The below-normal ENP activity since 1995 appears to be inversely related to the increased North Atlantic activity (Lander and Guard 1998; Landsea et al. 1998, 1999; Goldenberg et al. 2001; Bell and Chelliah 2006).

(iii) Impacts

None of the ENP tropical storms or hurricanes that formed in 2005 made landfall along Mexico's Pacific coast, which on average has at least one tropical storm and one hurricane landfall each year (Jauregui 2003). However, remnants of several tropical storms and hurricanes brought heavy precipitation to Mexico and Central America, as well as the Hawaiian Islands.

The first tropical cyclone of the season, Adrian, formed in mid-May from a tropical wave that crossed the Central American isthmus and intensified into a tropical storm on 18 May and to a hurricane the following day. Adrian reached peak intensity on 19 May, about 139 km southwest of El Salvador, with sustained winds of 70 kt. Poststorm reports from ships and reanalysis of satellite-derived intensities using the Dvorak (1984) technique indicate that the storm had weakened to a tropical depression just prior to landfall. Despite this rapid dissipation, heavy rainfall associated with the remnants of Adrian generated flooding and mudslides resulting in one storm-related death in Nicaragua (source: NOAA/NHC).

The other tropical cyclones that impacted Mexico were TS Dora, whose center of circulation did not cross the coast but passed just 65 km off Zihuatanejo, and H Otis that dissipated about 148 km northwest of Cabo San Lazaro. Otis generated tropical storm conditions in some coastal locations and heavy rainfall in the mountains of the southern Baja Peninsula.

The only tropical cyclone to impact the Hawaiian Islands during the 2005 season was MH Kenneth, which had the longest duration and reached the highest intensity of any tropical cyclone in the ENP basin in 2005. Kenneth initially became a tropical depression on 14 September, intensifying to a tropical storm on the 15th, and to a hurricane the following day. It reached its maximum intensity of 115 kt (minimal category 4 on the Saffir–Simpson scale) on 18 September, moved slowly east-northeastward and weakened to a tropical storm. Despite moving into a region of cooler SSTs, Kenneth reintensified into a hurricane and moved northwestward toward the island of Hawaii, finally dissipating just east of the island on 30 September. The remnants of Kenneth produced locally heavy rainfall, but there were no official reports of damages or injuries.

(iv) Environmental influences on the below-normal east North Pacific hurricane season

Tropical cyclone activity (both frequency and intensity) is influenced by several large-scale environmental factors, including SSTs, vertical wind shear in the mid- and upper-troposphere, the phase of the QBO in the tropical lower stratosphere, and the phase of the ENSO in the equatorial Pacific region (Whitney and Hobgood 1997). In 2005, above-normal vertical wind shear in the midtroposphere (850–200 hPa) was observed in the ENP basin during the 3-month (July–September) peak of the hurricane season (Fig. 4.14, top). Vertical wind shear anomalies exceeding 6 m s^{-1} occurred in the ENP basin's MDR, which is defined here between 10°–20°N and 90°–130°W (Fig. 4.14, red box). In addition to increased vertical wind shear, SSTs were below normal in the MDR during the peak of the hurricane season in 2005, with an area of −1° to −1.5°C SST anomalies off the coast of the Baja Peninsula (Fig. 4.14, bottom). These cool SST anomalies were located at the northern edge of the MDR, in a region of normally cooler water due to coastal upwelling and cold advection from the north associated with the California current.

Tropical cyclones in the ENP basin typically attain a higher intensity when the QBO is in its westerly

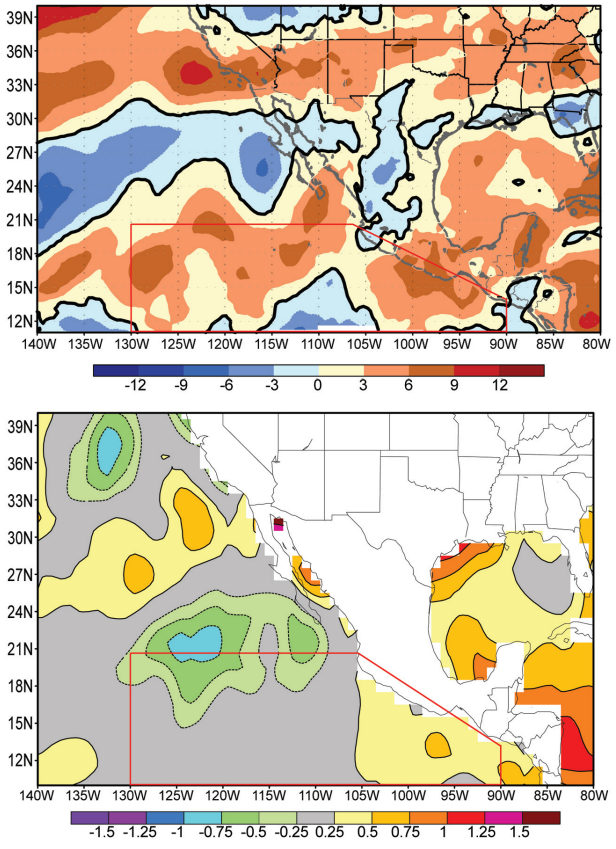

Fig. 4.14. (top) July–September 2005 200–850-hPa vertical wind shear anomaly (m s^{-1}; relative to 1979–2004 means; source: North American Regional Reanalysis dataset). (bottom) July–September 2005 sea surface temperature anomalies (°C) from NOAA's OI dataset (Reynolds and Smith 1994; Reynolds et al. 2002). The main development region for ENP hurricanes is the area delineated by the red box in both panels.

phase at 30 hPa in the tropical lower stratosphere, but there is also a corresponding decrease in the observed seasonal frequency of stroms (Whitney and Hobgood 1997). In 2005, the phase of the QBO anomaly was westerly, but with relatively weak zonal wind anomalies < 10 m s^{-1} at 30 hPa during the majority of the hurricane season (except in October when the phase of the 30-hPa zonal wind became easterly). Therefore, the activity in the ENP basin during 2005 was mixed relative to the phase of the QBO.

iv) Western North Pacific basin—S. J. Camargo[14]

Tropical cyclone [typhoon (TY)] activity in the western North Pacific (WNP) was slightly below average in 2005, with 25 tropical cyclones (TDs, TSs, and TYs), which was below the 1971–2004 climatological median of 31 (Fig. 4.15a). Only one of the tropical cyclones (TD 20W) failed to reach tropical storm intensity or higher. There were 24 NSs in 2005 (8 TSs and 16 TYs), which was below the climatological median of 26. The eight TSs in 2005 were also slightly below the climatological median of nine, and one of these (25W) was not officially named by the Joint Typhoon Warning Center (JTWC). The 16 TYs in 2005 equaled the climatological median, as did the four supertyphoons.

Other indices of tropical cyclone activity indicate a slightly below- to near-normal level of activity in the WNP in 2005. The 2005 ACE Index (Fig. 4.16a) was 298 × 10^4 kt^2 in 2005, which was slightly above the climatological median of 289.8 × 10^4 kt^2 and mainly due to the occurrence of four supertyphoons in 2005, which accounted for 75% of the total.

Monthly ACE values (Fig. 4.16b) were slightly above normal in the early season until September, and below normal during October–December. The June ACE Index value was the eighth highest in the historical record. In contrast, November and December ACE Index values were the 8th and 13th lowest,

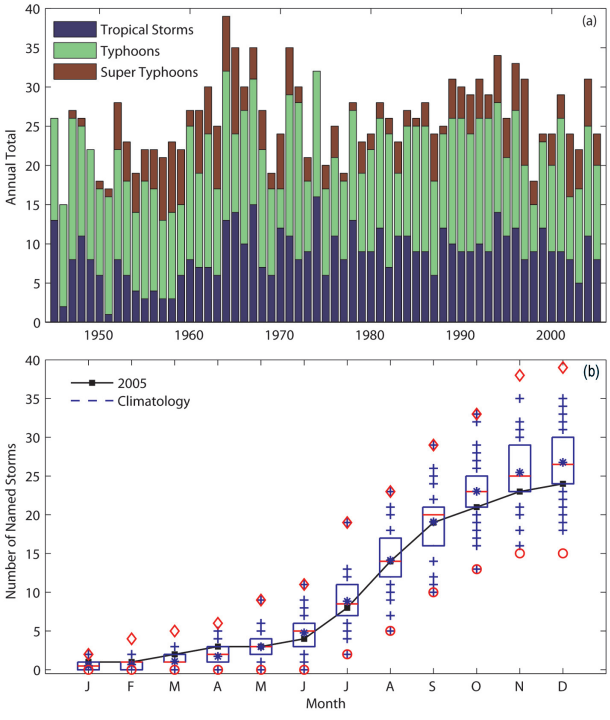

Fig. 4.15. (top) Number of tropical storms, typhoons and supertyphoons per year in the WNP for the period 1945–2005. (bottom) Cumulative number of named storms per month in the WNP: 2005 (black squares and line), and climatology (1971–2004) shown as box plots [box = interquartile range (IQR), red line = median, * = mean, + = values in top or bottom quartile, and diamonds (circles) = high (low) records in the 1945–2005 period]. [Source: JTWC]

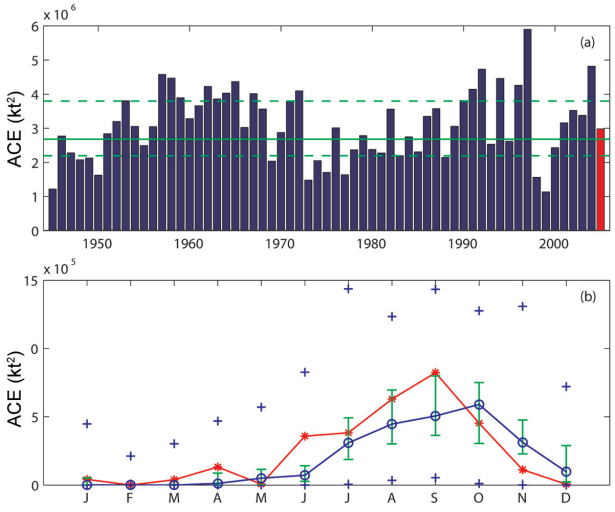

Fig. 4.16. (a) ACE Index (x 104 kt2) per year in the western North Pacific for the years 1945–2005. The solid green line indicates the median for the 1971–2004 base period (climatology), and the dashed green lines show the 25th and 75th percentiles. (b) ACE Index per month in 2005 (red line) and the median in the years 1971–2004 (blue line), where the green error bars indicate the 25th and 75th percentiles. In the cases of no error bars, the upper and/or lower percentiles coincide with the median. The blue plus signs (+) denote the maximum and minimum values during the period 1945–2005. [Source: JTWC]

respectively, in the historical record. The high June ACE value was due to typhoon Nesat, which was in the top 5% of the historical record of ACE per storm. The ACE index values of supertyphoons Longwang and Nabi were both in the top 10% of the historical record of ACE per storm.

The cumulative number of named storms per month (Fig. 4.15b) also shows an active early season (March–May), a slightly above-normal mid-season (August and September), and below-normal activity in the late season (October–December). The 131 NS days (days in which at least one tropical cyclone with tropical storm intensity or higher occurred) in 2005 was below the climatological median of 163.1 days. In contrast, the 29.25 days with intense typhoons (number of days having at least one typhoon with sustained winds ≥ 96 kt) was well above the climatological median of 20 days, and in the top 15% of the historical record.

WNP tropical storms and typhoons in 2005 had an average cyclogenesis position of 14.5°N, 138.4°E, which is slightly northwest of the climatological mean position (12.8°N, 143.5°E; 1.8° lat, 6.6° lon std dev). The average track position of all named storms was 20.4°N, 132.3°E, which is also slightly northwest of the climatological mean (19.0°N, 134.2°E). This shift to the northwest was due to several tropical cyclones that formed at higher latitudes (at or north of 20°N) and the absence of low-latitude (at or south of 15°N) tropical cyclones east of 155°E.

The 2005 WNP typhoon season was responsible for many fatalities and economic losses. Eight named tropical cyclones made landfall in China resulting in around 300 deaths and losses estimated at $3 billion USD (see also section 6f). Four cyclones affected Vietnam in 2005 (Damrey, Haitang, Longwang, and Kai Tak), and three strong typhoons (Talim, Haitang, and Longwang) made landfall in Taiwan. While Japan was struck by 10 tropical cyclones in 2004, only two (Nabi and Mawar) made landfall there in 2005. The high number of landfalls in China, Vietnam, and Taiwan (Fig. 4.17a) and the relative absence thereof in Japan were related to anomalous 500-hPa winds and vertical wind shear (Fig. 4.17b). Also present were anomalous low-level (850 hPa) easterlies, probably responsible for the absence of typhoons east of 150°E at low latitudes.

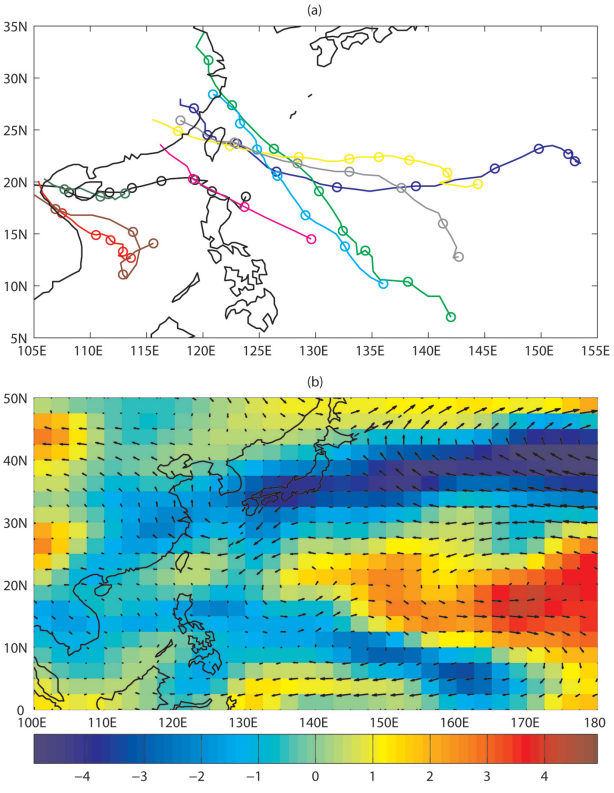

Fig. 4.17. (a) Observed tracks of tropical cyclones that made landfall in China, Taiwan, and Vietnam in 2005. (b) Anomalous 500-hPa winds (vectors) and anomalous vertical wind shear (m s^{-1}, shading) during July–October 2005.

v) Indian Ocean basins—K. L. Gleason[28]

(i) North Indian Ocean

The North Indian Ocean (NIO) tropical cyclone season extends from May to December, with two peaks in activity during May–June and November when the monsoon trough is climatologically positioned over tropical waters in the basin. Tropical cyclones in the NIO basin develop in the Bay of Bengal and the Arabian Sea typically between latitudes of 8° and 15°N and are usually short lived and weak, quickly moving into the subcontinent. However, severe cyclonic storms, with winds > 130 kt, can develop (Neumann et al. 1993).

Using reliable records from 1981 to 2000, a mean of less than one major cyclone (MCYC: sustained winds ≥ 96 kt), 1.6 cyclones (CYC: sustained winds ≥ 64 kt), and 4.75 NSs (sustained winds ≥ 34 kt) form each year in the NIO. The 2005 tropical cyclone season was near normal with one CYC and six NSs forming from January to December (Fig. 4.18, top). The sole CYC lasted at that strength for only 1 day, resulting in a below-average number of NIO cyclone days for 2005.

The estimated 2005 ACE Index for the NIO basin was 7×10^4 kt^2, which is less than half of the 1981–2000 mean of 19×10^4 kt^2 (Fig. 4.18, bottom). In fact, NIO activity has been below normal for the past 6 yr. This period follows four active tropical cyclone seasons with above-average ACE Index values during the late 1990s.

Tropical Cyclone Fanoos was the only hurricane-strength storm of the NIO season. Fanoos developed over the Bay of Bengal west of the Andaman Islands in early December and tracked west toward the southeast Indian coastline. On 9 December, CYC Fanoos briefly became a category 1 tropical cyclone before making landfall on the Tamil Nadu coast near Vedaranyam with 55-kt sustained winds. Two tropical storms also made landfall in 2005. Tropical storm 03B formed in early October along the Indian coastline and came ashore near the West Bengal state with 35-kt sustained winds. Tropical storm 04B formed near the Indian coast and made landfall in the Andhra Pradesh state in late October with sustained winds of 35 kt. Impacts from both of these storms were minimal.

In mid-September, a tropical depression developed over the South China Sea and moved inland over Thailand. Cyclonic Storm Pyarr, identified by the Indian Meteorological Department, moved into the Bay of Bengal and intensified into a tropical storm with estimated sustained winds of between 35 and 45 kt. Pyarr made landfall over the northeast Indian coast and quickly dissipated. This storm was not included in the NIO analyses for 2005 due to a lack of available track data and wind observations.

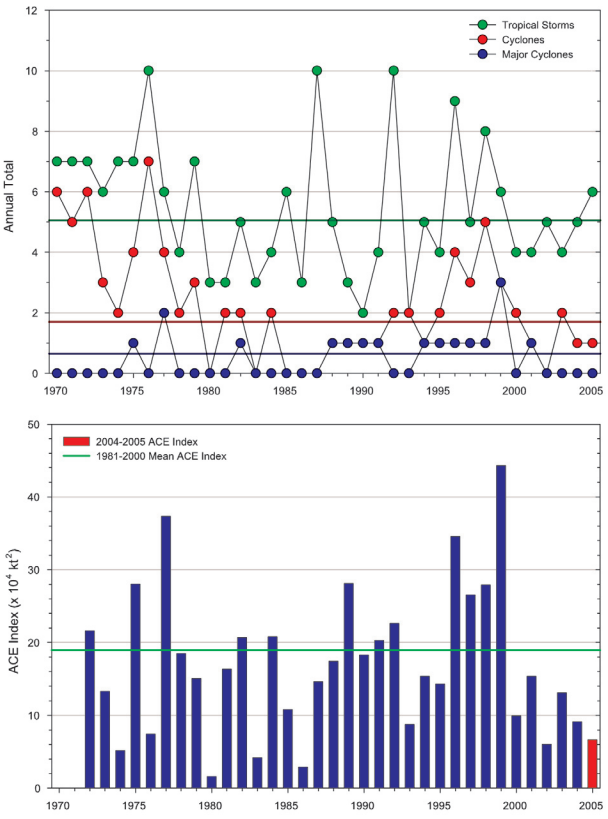

Fig. 4.18. Annual tropical cyclone statistics for the NIO 1970–2005. (top) Number of tropical storms, cyclones, and major cyclones. (bottom) Estimated annual ACE Index (x 10^4 kt^2) for all NIO tropical cyclones during which they were at least tropical storm or greater intensities (Bell et al. 2000). The ACE Index is estimated due to a lack of consistent 6-h sustained winds data for every storm.

(ii) South Indian Ocean

The tropical cyclone season in the South Indian Ocean (SIO) is typically active from December through April and officially extends from July to June, spanning two calendar years. The SIO basin extends south of the equator from the African coastline to 105°E, although most cyclones develop south of 10°S latitude. Cyclones in the SIO that remain east of 105°E are included in the Australian summary (see next section). The vast majority of SIO landfalling cyclones impact Madagascar, Mozambique, and the Mascarene Islands, including Mauritius. Due to a sparse historical observational record, and no centralized monitoring agency, the SIO is probably the least understood of all tropical cyclone basins

(Atkinson 1971; Neumann et al. 1993). As a result, the SIO statistics presented are incomplete, but are based upon verifiable information.

Using reliable data from 1980 to 2000, the SIO averages 2.7 MCYCs, 6.1 CYCs, and 11.95 NSs each year. During the 2004/05 season (from July 2004 to June 2005), the SIO tropical cyclone occurrences were near average with 3 MCYCs, 6 CYCs, and 14 NSs (Fig. 4.19, top). However, the estimated 2004/05 SIO ACE Index was 53×10^4 kt^2, which was less than half of the 1981–2000 average of 112×10^4 kt^2 (Fig. 4.19, bottom). This suggests a decreased intensity of tropical cyclones during this season, because both occurrences and mean cyclone duration (~4 days) were near average.

Three SIO tropical cyclones made landfall during the 2004/05 season. The first of these formed northeast of Madagascar in mid-January and moved west toward the African coastline. This TD became MCYC Ernest after intensifying to 100-kt sustained winds (category 3), while moving south over the warm waters of the Madagascar Channel. Ernest weakened slightly before brushing the southwestern coast of Madagascar on 22 January with 70-kt sustained winds. It then proceeded southeast over the cooler waters of the SIO and dissipated. Later in the month, Tropical Storm Felapi affected the same region. The combined effects from both systems caused widespread flooding across southern Madagascar. Earlier in the season, tropical cyclone 02S formed east-southeast of the Seychelles Islands in late October and moved west toward the African coastline. This storm briefly strengthened into a tropical storm before weakening and made landfall near Dar es Salaam, Tanzania, as a TD.

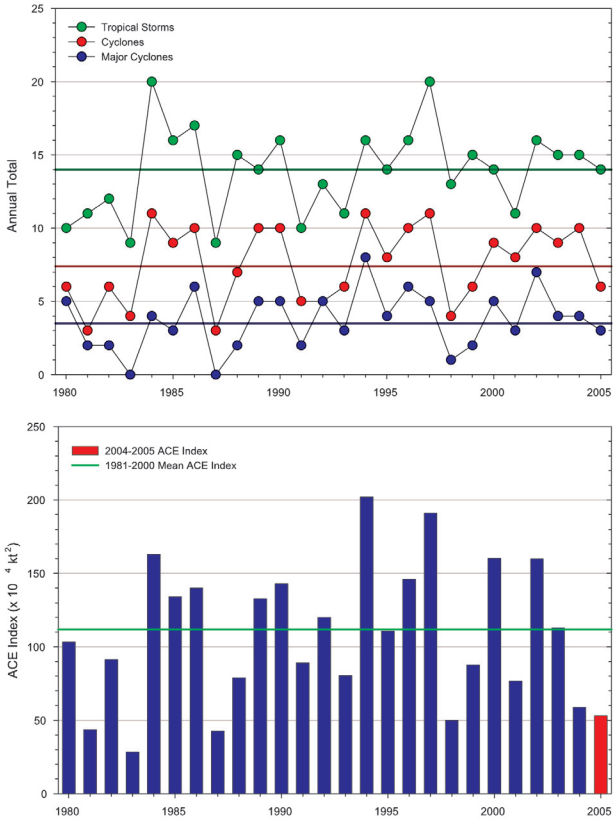

Fig. 4.19. Annual tropical cyclone statistics for the SIO 1980–2005. (top) Number of tropical storms, cyclones, and major cyclones. (bottom) Estimated annual ACE Index (x 10^4 kt^2) for all SIO tropical cyclones during which they were at least tropical storm or greater intensities (Bell et al. 2000). The ACE Index is estimated due to a lack of consistent 6-h sustained winds data for every storm.

The most intense SIO tropical cyclone of the 2004/05 season was MCYC Bento, with sustained winds of 140 kt. Bento developed in late November 2004, east-southeast of Diego Garcia in the central Indian Ocean, and quickly intensified. Fortunately, Bento remained well south of Diego Garcia and there were no significant impacts on the island. Bento was the first tropical cyclone on record in the SIO to reach category 5 intensity equatorward of 10°S latitude.

CYC Adeline-Juliet, formed near the Cocos Islands in the southeast Indian Ocean during early April 2005 and began its westward movement toward the central SIO. Adeline-Juliet reached peak intensity of 120-kt sustained winds (category 4) on 8 April while tracking west-southwest to within 213 km of Rodrigues Island. It then quickly dissipated as it moved southward into an unfavorable environment of strong vertical shear, drier air, and cooler SSTs.

vi) South Pacific basins—M. J. Salinger,[80] A. B. Watkins,[90] and S. M. Burgess[12]

(i) Southwest Pacific

The 2004/05 southwest Pacific tropical cyclone season had a climatological average nine tropical storms east of 150°E (Fig. 4.20), four of which reached MCYC strength. All but one of the nine tropical cyclones originated east of the date line (Fig. 4.21), and all occurred between December and April.

The most devastating tropical cyclones of the 2004/05 season were Meena, Nancy, Olaf, and Percy. These systems all occurred in February in association with an active phase of the Madden–Julian oscillation.

Judy was the first tropical cyclone of the season (25 December) and brought torrential rainfall to parts of

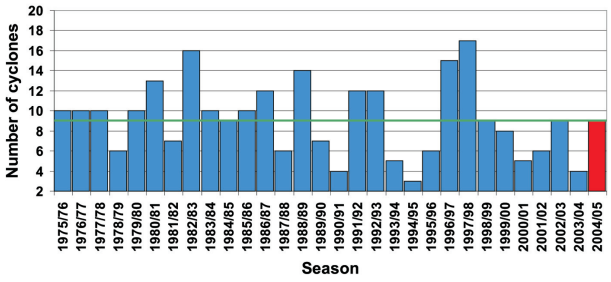

FIG. 4.20. The number of southwest Pacific tropical cyclones for the 2004/05 season (solid red bar) compared to frequencies during the past 30 years. The horizontal green line indicates the 30-yr average (Not including Ingrid, which originated west of 150°E).

the Tuamotu Islands, French Polynesia. CYC Kerry developed northeast of Vanuatu on 6 January, passing over the Pentecost and Malekula Islands the next day, with pressures as low as 987 hPa and maximum sustained wind speeds of 90 kt. Lola affected the region near Tonga from 31 January through 2 February, with strong winds at Fua'amotu Airport.

MCYC Meena formed east of Samoa on 3 February and tracked toward the southern Cook Islands. Estimated maximum sustained wind speeds reached 125 kt, with gusts to 155 kt. Tropical storm–force winds occurred at Mauke on 6 February with pressures as low as 986 hPa. Gale-force winds and gusts to 62 kt occurred in Rarotonga on the same day, preceded by about 100 mm of rain.

MCYC Nancy affected the northern Cook Islands from 13 to 15 February tracking south, forcing Aitutaki residents and tourists into shelters on 15–16 February. Estimated sustained maximum winds in Nancy reached 125 kt, while storm-force winds gusted to 88 kt in Rarotonga with reports of 100 kt elsewhere. Heavy rainfall, pressure as low as 988 hPa, and high seas also accompanied the storm. In Aitutaki, trees were uprooted, roofs damaged, and low-lying areas flooded. Waves caused widespread destruction along the northern and eastern coasts of Rarotonga. The island of Mangaia was also badly hit.

Olaf was named on 13 February, and reached MCYC strength with 145-kt maximum sustained winds. Observed winds exceeded 65 kt in Samoa on 16 February, damaging numerous structures. Gales buffeted the northern and southern Cook Islands on 17 February, with gusts to 51 kt in Rarotonga.

MCYC Percy, with maximum sustained winds reaching 140 kt came next. Gales, storm surge, and high tides affected Tokelau on 26 February, where Percy was reportedly the worst tropical cyclone in living memory. Many homes were damaged and roads washed out, with water up to 1 m deep in some areas.

Rae followed (near the southern Cook Islands) on 6 March, but remained weak. Finally, Shelia formed east of Niue on 22 April and tracked southeast, with maximum sustained winds reaching 35 kt.

(ii) Australian basin

As with the 2003/04 season, the 2004/05 Australian basin TC season saw only six TCs between 105° and 160°E, compared with a long-term average of approximately 10. Three were classified as severe tropical cyclones.

The most severe, TC Ingrid, occurred between 5 and 16 March (Fig. 4.22). Ingrid formed in the Coral Sea south of Papua New Guinea and tracked first east- then westward across Cape York Peninsula and through offshore islands off the Northern Territory coast, before making landfall in the far north of Western Australia. Ingrid is the only TC in Australia's recorded history to impact the coastline of three different states or territories as a severe tropical cyclone (category 3 or above on the Australian tropical cyclone warning scale). Fortunately, some weakening before its coastal crossings resulted in only modest damage.

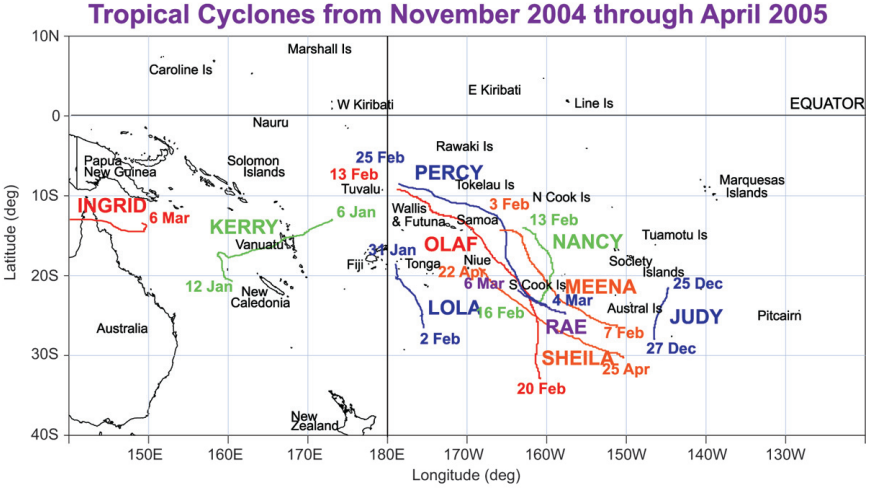

FIG. 4.21. Southwest Pacific tropical cyclone tracks for the 2004/05 season (including Ingrid).

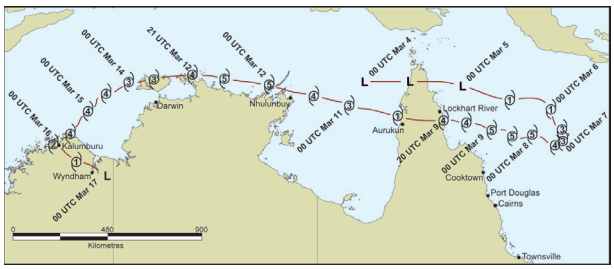

Fig. 4.22. Observed track of Tropical Cyclone Ingrid along the northern coast of Australia. [Courtesy: M. Foley and M. Lesley, Australian Bureau of Meteorology (BOM)]

d. Pacific intertropical convergence zone—A. B. Mullan[59]

Prominent rainfall and cloudiness maxima and OLR minima are associated with the Pacific ITCZ and the SPCZ. The Pacific ITCZ has its main branch in the Northern Hemisphere between 5° and 10°N, where it is strongest during June–August (Fig. 4.25). Between December and February, the ITCZ branches south of the equator, near 5°S, and is associated with the monsoon trough near Australia. Convection frequently extends northward from the monsoon trough across the equator in the region of the Maritime Continent. The southern ITCZ rarely extends

THE RECORD BREAKING 2005 ATLANTIC HURRICANE SEASON—G. D. Bell,[5] E. Blake,[8] K. C. Mo,[58] C. W. Landsea,[44] R. Pasch,[65] M. Chelliah,[15] S. B. Goldenberg,[29] And H. J. Diamond[19]

The 2005 Atlantic hurricane season was unprecedented and broke many tropical cyclone records. The season featured a record 27 tropical storms (previous record of 21 in 1933), a record 15 hurricanes (previously 12 in 1969), a record three category 5 hurricanes (previously two in both 1960 and 1961), a record estimated ACE Index (Bell et al. 2000) of 285% of the median, and a record ACE value of 131% of the median from named storms forming outside the MDR. The MDR is the tropical Atlantic and Caribbean Sea south of 21.5°N (Fig. 4.7, green box). The season also featured a record 15 named storms making landfall in the Atlantic basin. Seven of these made landfall in the United States, including a record four landfalling major hurricanes (categories 3–5 on the Saffir–Simpson scale; Simpson 1974). Also, a record seven named storms occurred during June–July, and a record 10 late-season storms formed after 1 October. Seven storms became major hurricanes during 2005, one shy of the 1950 record.

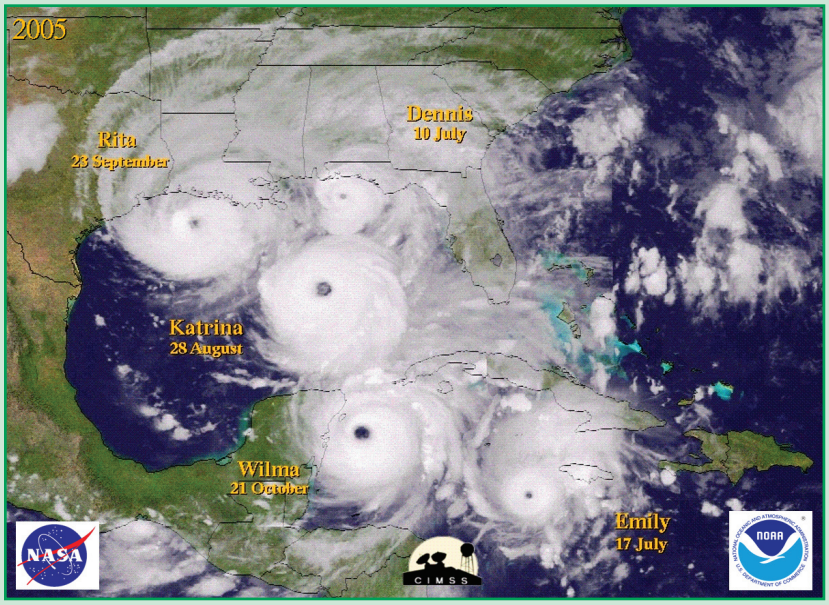

Fig. 4.23. Satellite montage of U.S. landfalling hurricanes. [Courtesy: C. Velden, University of Wisconsin—Madison, Cooperative Institute for Mesoscale Meteorological Studies (CIMMS)]

Two tropical storms, two hurricanes, and four major hurricanes struck the United States during 2005 (Fig. 4.23). These totals reflect the effects of H Ophelia on the Outer Banks of North Carolina.The devastating impacts of H Katrina on the central Gulf Coast in late August, one of the worst natural disasters ever to strike the United States, made the 2005 season the costliest season in the country's history, conservatively estimated at over $100 billion USD. Elsewhere, three tropical storms and three hurricanes (including Wilma) struck Mexico, one tropical storm made landfall in the Dominican Republic, and one hurricane struck Nicaragua. In Guatemala, Stan claimed over 1000 lives in mudslides and flooding. Wilma was the costliest natural disaster in Mexican history with estimated damage at $1–3 billion USD, eight deaths, and a reported 1637 mm (64 in.) of precipitation recorded on Isla de Mujeras. The number of additional monthly and individual records is too numerous to list here, but several are of particular note:

- Since the inception of the current naming system in 1953, this year was the first time the Greek letter naming convention was used.
- Dennis became the most intense hurricane on record before August when a central pressure of 930 hPa was recorded.
- Emily eclipsed the record set by Dennis for the lowest pressure recorded for a hurricane before

eastward of about 160°W, except during March and April when it can reach 90°W. High-resolution Tropical Rainfall Measuring Mission (TRMM) rainfall data show that the southern ITCZ is particularly prominent east of 160°W in La Niña years, such as 1999/2001.

Near the date line, the southern ITCZ merges with the SPCZ, which extends southeastward across the subtropical South Pacific. The SPCZ is most active in austral summer (December–February) and is located in a region of strong SST gradient south of the maximum SSTs. In contrast, the Northern Hemisphere ITCZ is located near the axis of maximum SSTs (Vincent 1998).

The northern ITCZ was continuous across the Pacific from 140°E to 90°W in almost all months except February (Fig. 4.25, top). Also during February, the SPCZ was extremely active from about 160°E to 160°W in association with more extensive equatorial westerlies and several tropical cyclones (see previous section). From May to August the northern ITCZ was positioned slightly equatorward of its normal location, and during June and August it was particularly active in the far eastern tropical Pacific between 120°W and 90°W (Fig. 4.25, bottom).

August when its central pressure reached 929 hPa.

- Vince was the first tropical cyclone in recorded history to strike the Iberian Peninsula. While Alberto (1988) was the most northerly and Ginger (1967) the most easterly, Vince was the most northeasterly, and was also the furthest east when it became a hurricane.
- Wilma's central pressure dropped to 882 hPa, which was the lowest pressure ever measured in the Atlantic basin, eclipsing the old record of 888 hPa set by H Gilbert in 1988.
- Zeta tied Alice (1954) for latest naming (30 December), and was the longest lived into January (6 January).

The activity of the 2005 season is attributed to four main factors: 1) long periods of anomalous upper-level convergence and suppressed convection over the central tropical Pacific, reminiscent of La Niña conditions; 2) record warm sea surface temperatures across the MDR; 3) the ongoing tropical multidecadal signal; and (4) exceptionally conducive upper-level and lower-level wind and air pressure patterns over the western Atlantic and Gulf of Mexico.

NOAA's ACE Index is a measure of seasonal activity that accounts for the combined strength and duration of tropical storms and hurricanes during the season (Fig 4.24; Bell et al. 2000). ACE is calculated by summing the squares of the 6-h maximum sustained wind speed in knots for all periods while the system is a tropical storm, subtropical storm, or hurricane. The 2005 ACE value was a record 249 $\times 10^4$ kt^2 (285% of the 1951–2000 median value). The 2005 season marks a continuation of the current active hurricane era that began in 1995. The historical time series of the ACE Index indicates large multidecadal fluctuations in seasonal activity (Goldenberg et al. 2001; Bell and Chelliah 2006). During the 11-yr period from 1995 to 2005, seasons have averaged 14.7 TSs, 8.4 Hs, and 4.1 MHs, and every season has been classified by NOAA as above normal except for the two El Niño years of 1997 and 2002. In contrast, seasons during the below-normal period 1971–94 averaged only 9 TSs, 5 Hs, and 1.5 MHs, with only three seasons classified as above normal (1980, 1988, 1989). These large differences between the above-normal and below-normal eras result almost entirely from differences in the number of tropical storms that form in the MDR and eventually become hurricanes and major hurricanes (Landsea 1993; Goldenberg et al. 2001).

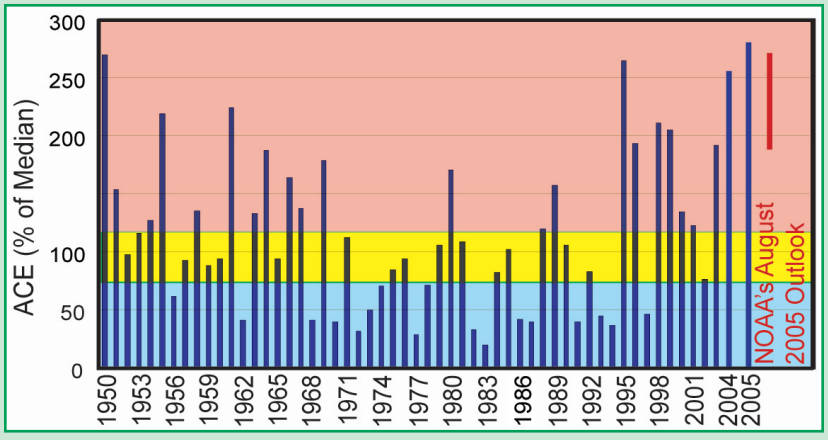

Fig. 4.24. ACE Index expressed as percent of the 1951–2000 median value. Season types are indicated by the background shading, with pink, yellow, and blue approximating above-, near-, and below- normal seasons, respectively.

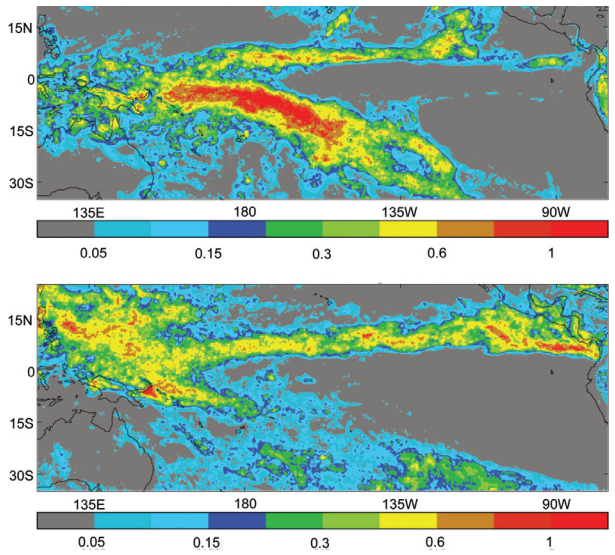

Fig. 4.25. Average rainfall rate (mm h^{-1}) from TRMM 0.25° analysis for (top) February and (bottom) August 2005. Contours are unevenly spaced at 0.05, 0.10, 0.15, 0.20, 0.30, 0.40, 0.60, 0.80, and 1.00 mm h^{-1}.

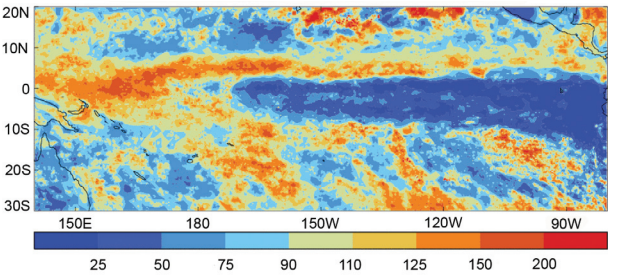

Fig. 4.26. Annual average rainfall rate (mm h^{-1}) from TRMM 0.25° analysis for 2005, as a percentage of the 1998–2004 mean.

For the year as a whole, high-resolution TRMM rainfall data (0.25° latitude × 0.25° longitude grid) suggest that precipitation was slightly above the 1998–2004 average in the northern ITCZ (Fig. 4.26), and also in the southern ITCZ and SPCZ to about 160°W.

5. THE POLES—A. M. Waple[89], Ed.

a. Overview—A. M. Waple[89] and J. Richter-Menge[74]

The permanent presence of sea ice, ice sheets, and continuous permafrost are unique features of the polar regions. The Arctic is further distinguished because it sustains human and wildlife populations in a harsh environment, as documented in the Arctic Climate Impact Assessment published in November 2004 (online at www.acia.uaf.edu). These characteristics amplify the impact of climate change on the region's physical, ecological, and societal systems. Such impacts reach beyond the Arctic region. For instance, studies are underway to determine the extent to which the loss of sea ice cover and the conversion of tundra to larger shrubs and wetlands, observed to have occurred over the last two decades, have impacted multiyear persistence in the surface temperature fields, especially in the Pacific sector.

In this section, observations that indicate continuing trends in the current state of physical components of the Arctic system, including the atmosphere, ocean, sea ice cover, and land, are discussed. The temporal extent of the data provides a multidecadal perspective and confirms the sensitivity of the Arctic to changes in the global climate system. The destabilization of several known relationships between climate indices (e.g., Arctic Oscillation) and Arctic physical system characteristics (e.g., continued reduced sea ice cover and increased greenness of the tundra) presents an intriguing and significant puzzle with respect to the contemporary global climate system.

It was one of the warmest years on record for Greenland, with an especially warm and foggy spring. Surface temperature and ice melt are discussed for Greenland in the context of a warming trend over the nation.

Also, trends and observations in temperature, sea ice, and stratospheric ozone depletion are discussed with respect to Antarctica. As the continent with more than 70% of Earth's freshwater storage, trends in Antarctic climate are of critical importance in determining the long-term impact of climate change.

b. Arctic—J. Richter-Menge,[74] J. Overland,[62] A. Proshutinsky,[68] V. Romanovsky,[77] J. C. Gascard,[25] M. Karcher,[37] J. Maslanik,[52] D. Perovich,[66] A. Shiklomanov,[83] and D. Walker[87]

1) Atmosphere

(i) Circulation regime

The annually averaged AO index in 2005 was slightly negative, continuing the trend of a relatively low and fluctuating index that began in the mid-1990s (Fig. 5.1). This follows a strong positive pattern from 1989 to 1995. Current characteristics of the AO are more consistent with the period from the 1950s to the 1980s, when the AO switched frequently between positive and negative phases.

(ii) Surface temperatures

In 2005, annual average surface temperatures over land areas north of 60°N remained above the mean value for the twentieth century (Fig. 5.2), as they have since the early 1990s. Figure 5.2 also shows warm temperatures in the 1930s and early 1940s, possibly suggesting a longer-term oscillation in climate. However, a detailed analysis shows different proximate